Mast Cells-derived Exosomes Promote the Development of Experimental Cerebral Malaria

Kunhua Huang
Guangdong Pharmaceutical University
Xin Zhang
Guangdong Pharmaceutical University
Li Huang
Guangdong Pharmaceutical University
Hang Lin
Guangdong Pharmaceutical University
Ziyi Yu
Guangdong Pharmaceutical University
Xiaobo Li
Guangdong Pharmaceutical University
Xiao Bo Liu
Guangdong Pharmaceutical University
Qiang Wu
Guangdong Pharmaceutical University
Yongfei Wang
Jinan University
Jie Wang
Guangdong Pharmaceutical University
Xiaobao Jin
Guangdong Pharmaceutical University
Xiaoying Han
McGill University
Hongzhi Gao
2nd Affiliated Hospital of Fujian Medical University
Rongtuan Lin
McGill University
Shan Cen
Chinese Academy of Medical Sciences
Zhenlong Liu
McGill University
Bo Huang (hb@gdpu.edu.cn)

Guangdong Pharmaceutical University

Research

Keywords: Cerebral malaria, Mast cells, Exosome, Blood brain barrier, bEnd.3 cells

Posted Date: December 10th, 2020

DOI: https://doi.org/10.21203/rs.3.rs-121995/v1

Abstract

Background: Cerebral malaria (CM) is a severe neurological manifestation caused by *Plasmodium* infection, with high morbidity and mortality rate, and long-term cognitive impairments in survivors. Exosomes are cell-derived nano-vesicles secreted by virtually all types of cells and serve as mediators of intercellular communication. Studies have demonstrated that mast cells (MCs) play a critical role in mediating malaria severity, however, the potential functions and pathological mechanisms of MCs-derived exosome (MCs-Exo) impacting on CM pathogenesis remain largely unknown.

Methods: Herein, we utilized an experimental CM (ECM) murine model (C57BL/6 mice infected with *P. berghei* ANKA), and then intravenously (i.v.) injected MCs-Exo into ECM mice to investigate the effect of MCs-Exo on ECM pathogenies. We also used an *in vitro* model by investigating the pathogenesis development of brain microvascular endothelial cells line (bEnd.3 cells) upon MCs-Exo treatment after *P. berghei* ANKA blood-stage soluble antigen (*Pb*Ag) stimulation.

Results: MCs-Exo were successfully isolated from culture supernatants of mouse MCs line (P815 cells) stimulated with *Pb*Ag, characterized by spherical vesicles with the diameter of 30–150 nm, expressing of typical exosomal markers, including CD9, CD81, and CD63. *In vivo* and *ex vivo* tracking showed that DiR-labeled MCs-Exo were taken up by liver and brain tissues after 6 h of i.v. injection. Compared with naive mice, ECM mice exhibited higher numbers of MCs and higher levels of MCs degranulation in various tissues (e.g., brain, cervical lymph node, and skin). The present of MCs-Exo dramatically shortened survival time, elevated incident of ECM, exacerbated liver and brain histopathological damage, promoted Th1 cytokine response, and aggravated brain vascular endothelial activation and blood brain barrier breakdown in ECM mice. Interestingly, compared with bEnd.3 cells stimulated with *Pb*Ag, the treatment of MCs-Exo led to decrease of cells viability, increase the mRNA levels of Ang-2, CCL2, CXCL1, and CXCL9, and decrease the mRNA levels of Ang-1, ZO-1, and Claudin-5.

Conclusions: Thus, our data suggest that MCs-Exo could promote pathogenesis of ECM in mice.

Introduction

Despite incremental progress in the control and treatment of malaria that transmitted by *Anopheles* mosquitoes harboring *Plasmodium* parasites, this disease remains one of the most serious life-threatening problem worldwide, with an ~228 million cases and ~405,000 deaths in 2018 [1]. Cerebral malaria (CM), a common type, severe and lethal complications of *P. falciparum* infection, occurred in ~1% of malaria infections annually and was responsible for more than 90% of malaria deaths [2]. CM patients usually exhibited severe clinical manifestations (e.g., seizures, convulsions, hemiplegia, delirium, epilepsy, and coma). It was reported that the fatality rate of CM ranged from 15% to 25%, and ~25% of CM survivors suffered a long-term neurological impairment in [3], despite treatment with highly effective anti-malarial drugs (e.g., the artemisinin-based combination therapies). Currently, restriction of routine malaria control (e.g., long-lasting insecticide–treated nets and indoor residual spraying) in Africa caused by

COVID-19 pandemic [4,5], emergence and spreading of anti-malaria drug resistance [6,7], as well as ineffective malaria vaccine [8] present a major challenge for malaria control and CM treatment, which makes it to be much more essential to elucidate the pathological mechanisms of CM. Generally, accumulating evidences indicated that infected red blood cells (iRBC) sequestration within the cerebrovasculature, accompanied by blood-brain barrier (BBB) disruption, overpowering neuro-inflammation responses, and neurological damage possibly contribute to the development of CM pathogenesis [2]. However, the pathological mechanisms of CM pathogenesis remain incompletely understood. It is well known that the BBB integrity is comprised of brain microvascular endothelial cells, a basement membrane, pericytes and astrocytes endfeet, thereby minimizing local inflammation and neuronal damage [9]. Currently, the destruction of BBB integrity was one of the key events that aggravated the pathogenesis of CM disease, and was closely associated with the appearance of long-term neurological signs in the survivors [10]. Nevertheless, the pathological features that underlying how BBB disruption is triggered when CM occurs have not been adequately investigated or characterized.

Mast cells (MCs) are granule-containing cells located in virtually every organ. Due to characteristics of widespread distribution in tissues, immediate release of massive mediators, and repetition of degranulation/regranulation cycle, MCs are not only crucial players in allergy and anaphylaxis [11], but also have a pivotal role in host defense against various kinds of parasites [12,13]. Many studies had demonstrated that MCs were implicated in malaria severity [14], although only one study showed that MCs were not associated with ECM pathogenesis as MCs-deficient C57BL/6 mice after *P. berghei* ANKA strain (*Pb*ANKA) infection developed an ECM disease similar to wild-type mice [15]. Serial reports demonstrated that elevated number of MCs and degree of MCs degranulation were positively associated with higher parasitamia, more vascular permeability and severe disease severity [16,17]. Notably, further analysis displayed that TNF released from MCs has crucial roles in host defense against *Pb*ANKA infection in murine model [18]; whereas MCs-derived Flt3 or histamine contrarily aggravated tissues damage, promoted intestinal permeability, and accelerated onset of ECM and mortality in *Pb*ANKA-infected C57BL/6 mice [19-21]. Collectively, these evidences have strong implications for a controversial role of MCs in regulating the malaria pathogenesis, in which protective or pathologic outcomes in malaria severity possibly caused by release of different kinds of mediators [22].

Exosomes, as extracellular nano-vesicles with diameter of 30–150 nm, are secreted by virtually all types of cells [23]. Given that harboring a variety of biomolecules (e.g., lncRNAs, microRNAs, proteins, and lipids) and transferring biomolecule information to neighboring cells or distant organs, exosomes are found to have an ability of achieving cell-cell communication under physiological and/or pathological conditions [23]. Currently, the function and potential application of exosomes derived from host cells and pathogens in progression of CM diseases has evoked increasing interest [24-26]. Accumulating evidences have demonstrated that exosomes or exosome-like vesicles derived from erythrocytes (or reticulocytes) infected with *P. falciparum* have multiple biological functions, including enhancing parasite transmission [27], altering vascular function [28], and so on. In addition, immunization with exosomes from a non-lethal strain of *P. yoelii* 17X-infected reticulocytes plus CpG ODN 1826 protected mice from a lethal strain of *P. yoelii* 17XL infection, as indicated by eliciting IgG2a and IgG2b antibodies, promoting host survival

time and clearance of parasites [29]. A serial of studies had demonstrated that several kinds of MCs (including bone marrow MCs, peritoneal MCs, and MC lines P815 and MC/9) constitutively secreted exosomes [30,31], and these exosomes were found to mediate function or activity of B cells, T cells, DCs and neurons [32,33], allergic reactions [34], and tumor cell metastasis [35]. To date, the pathological features underlying how MCs-derived exosomes (MCs-Exo) modulate the pathogenesis of CM is unknown. In this study, we utilized a widely-used and exclusive model of ECM by infecting susceptible C57BL/6 mice with *Pb*ANKA, and then intravenously (i.v.) injected MCs-Exo into ECM mice. We also used an in *vitro* model by investigating the pathogenesis development of brain microvascular endothelial cells line (bEnd.3 cells) upon MCs-Exo treatment after *Pb*ANKA blood-stage soluble antigen (*Pb*Ag) stimulation. Our finding could update the current understanding of the roles of MCs-Exo in ECM pathogenesis.

Methods

Animals, Parasite, and Ethics Statement

Female C57BL/6 outbred mice aged ~6 weeks and weighted ~20g were obtained from the Medical Laboratory Animal Center of Guangdong, and housed in pathogen-free environment in the Laboratory Animal Center of Guangdong Pharmaceutical University, PR China. *Pb*ANKA strain was routinely maintained in liquid nitrogen, and intraperitoneally (i.p.) injected into healthy female C57BL/6 mice that served as parasite donor for the infection of experimental groups. The experimental protocols were performed with the approval of the Animal Ethics Committee of Guangdong Pharmaceutical University (No. gdpulac2020023), and confirmed to the National Guidelines for the Care and Use of Laboratory Animals.

Preparation of *Pb*ANKA blood-stage soluble antigen (*Pb*Ag)

Blood were harvested from *Pb*ANKA infected-C57BL/6 mice (~40% parasitemia). After the leucocytes were removed from blood using Leukocyte Removal Filter (Beijing ZKSK Technology Co., Ltd, China), iRBCs were isolated using density gradient centrifugation with 60% Perco ll solution. The iRBCs were extracted in 0.01% saponin lysis buffer for 30 min at 4°C, followed by the centrifugation at 10,000 rpm for 1 min. The blood-stage parasites were harvested by centrifugation at 10,000 × g for 1 min, followed by 4X washes with PBS to get rid of soluble red blood cells proteins. The whole parasites were suspended in PBS and disrupted with a sonicator probe at 80W on ice. After filtrating through 0.2um Whatman filter devices, *Pb*Ag was quantitated using BCA kit assay and stored at −80 °C until use.

Mouse MCs line culture and challenge, Exosome Purification

The mouse mast cells line (P815 cells) were kindly provided by Stem Cell Bank, Chinese Academy of Sciences (Shanghai, China), and cultured in RPMI-1640 medium (GIBCO, No. 31800022#) containing FBS (10%), $NaHCO_3$ (1.5g/L), glucose (2.5g/L), sodium pyruvate (0.11g/L), penicillin (100 U/mL), and streptomycin (100 μg/mL) in 75-cm^2 tissue culture flasks at 37 °C in 5% CO_2 and 95% air atmosphere.

When the cells attained a density of 10^6 cells/mL, the P815 cells were washed with PBS twice and immediately exposed to *Pb*Ag (20 μg/mL) in the serum-free basal medium for 6 h. The culture supernatants were harvested by centrifugation at 2,000 r/min and 4°C for 10 min. Exosomes from the supernatant of the P815 cells were purified using an exosome isolation kit (Invitrogen, USA), according to the manufacturer's instructions.

MCs-Exo analyzed by TEM, Western Blotting, and NanoSight assays

The MCs-Exo were suspended in 2% glutaraldehyde, and then adsorbed at copper grids for 5 min at room temperature. Samples were negatively stained with 3% (w/v) aqueous phosphotungstic acid for 1 min and observed using a FEI Tecnai G2 Sprit Twin transmission electron microscope (TEM; FEI, USA). The size and the concentration of MCs-Exo suspended in PBS were analyzed using NanoSight NS300 (Malvern Instruments, UK). In addition, the exosomal markers such as CD9, CD81, and CD63 of MCs-Exo were detected by Western Blotting assay. In brief, after the protein levels of MCs-Exo were determined by using a bicinchoninic acid protein assay kit (Beyotime, China), MCs-Exo were lysed in a western blotting lysis buffer, and separated using 10% SDS-PAGE, electrophoretically transferred onto a polyvinylidene fluoride blotting membrane (GE Healthcare Life Sciences, UK), and then blocked using 5% skimmed milk. The membranes were incubated with anti-mouse CD63, CD9 and CD81 antibody (BD Biosciences, USA) overnight at 4°C. Anti-mouse antibodies conjugated with horseradish peroxidase (HRP) (Jackson Immunoresearch Labs Inc., USA) were used as secondary antibodies. Membranes were visualized via an enhanced chemiluminescence (ECL) chemiluminescent detection system (Amersham, USA).

In vivo and *ex vivo* tracking of MCs-Exo

For labeling MCs-Exo, 5 μL of DiR dye (2mg/mL in DMSO; Life Technologies, USA) was completely mixed with 200 μg MCs-Exo in 200 μL of PBS for 30 min in the dark. The mixture was centrifuged at 120,000 × g for 90 min to remove the unincorporated DiR dye, and the final pellet was resuspended in 200 μL of PBS. After being anaesthetized by intraperitoneal (i.p.) injection with chloral hydrate, the naïve C58BL/6 mice intravenously (i.v.) injected with 5 μL of the DiR-labeled MCs-Exo in PBS to verify the distribution of MCs-Exo in mice. After 6 h injection, living animals were imaged by using the Maestro2 In-Vivo Imaging System (Maestro, USA). Upon completion of live imaging, the animals were sacrificed by CO_2 asphyxiation, and major organs were harvested for fluorescence imaging.

MCs-Exo treatment in ECM model

To determine whether MCs-Exo mediate pathogenesis of ECM in mice, the experimental procedures were carried out in the following. Female C57BL/6 outbred mice were divided into 4 different groups: the uninfected mice that did not receive MCs-Exo treatment were used as negative controls (naïve group); the uninfected mice received daily i.v. injection of MCs-Exo (50 μg/mouse) as MCs-Exo group; the mice were only injected i.p. with 10^6 *Pb*ANKA-iRBCs as *Pb* group; whereas mice subjected to *Pb*ANKA infection received daily i.v. injection of MCs-Exo (50 μg/mouse) as *Pb+*MCs-Exo group. Parasitemia in different groups was monitored daily by Giemsa-stained thin blood smears of tail blood. The mice were evaluated

daily regarding survival time and neurological signs of ECM in mice. Once the *Pb*ANKA-infected mice exhibited neurological manifestations (e.g., coma, loss of reflex, prostration, paralysis, and convulsions), and usually moribund within 6-9 days postinfection (p.i.), these mice were classified as ECM mice.

Toluidine blue staining for MCs

Mice in different groups were sacrificed by CO_2 asphyxiation, and major organs (cervical lymph node, skin, and brain) were harvested, immediately fixed in 4% neutral buffered formalin for 48 h, embedded in paraffin, and then cut into 5-μm-thick sections using a Leica microtome (Leica, Germany). After being deparaffinized and rehydrated, these sections were stained with 0.5% toluidine blue (Sigma-Aldrich, USA) for 12 h. The positive MCs that show deep blue-purple staining were visualized and analyzed under a light DM 2500B microscope (Leica, Germany). The number of MCs and level of degranulated forms in tissues was calculated as described protocols in our previous report [17].

Histopathological analysis

Mice in different groups were euthanatized by CO_2 asphyxiation, and their liver and brain tissues were removed, immersed in 4% neutral buffered formalin for 48 h, and then embedded in paraffin. Five-millimeter paraffin sections were stained with haematoxylin and eosin (H&E) dye, and analyzed for histopathological changes under a light microscope at a magnification of ×200 (Leica DM 2500B, Germany). To assess liver tissue damage, the number of inflammatory foci per field in liver tissues were calculated at a magnification of ×200 under a light microscopy.

ELISA assay for determining Th1 cytokines and AST/ALT in sera

Blood were harvested from mice in different groups, level of Th1 cytokines (IFN-γ, TNF-α, IL-6, and IL-1α), and liver damage markers (AST and ALT) in sera were measured by Enzyme-linked immunosorbent assay (ELISA) kits according to manufacturer's protocols (Gusabio, China). The concentration of cytokines or AST/ALT was calculated by measuring the absorbance at a wavelength of 450 nm using a Model Microplate Reader (iMark, USA) and comparing to standard curves generated from recombinant standard proteins.

Immunohistochemistry for ICAM-1 and VCAM-1 in brain tissue

After being deparaffinized and rehydrated in distilled water, five-millimeter paraffin brain slices were placed in odium citrate buffer for 10 minutes at 95 °C to achieve antigen retrieval. The slices were incubated with 3% H_2O_2 in dH_2O to inhabit the endogenous peroxidase activity, and then place in 10% normal goat serum at 37 °C for 10 min to block non-specific binding. Slices were incubated with polyclonal mouse anti-ICAM-1 antibody (1:200 dilution; Servicebio, China) or polyclonal mouse anti-VCAM-1 antibody (1:200 dilution; Servicebio, China) for 1 h at 37°C. After being rinsed three times with PBS, slices were then incubated with biotinylated goat anti-mouse IgG (5 mg/mL, 1:200 dilution; Zhongshan, Beijing, China) for 1 h in darkness at room temperature. The slides were washed three times

with PBS, exposed to avidin–biotin–peroxidase complex (Zhongshan, Beijing, China) for 20 min at 37°C, and then counterstained with hematoxylin. The positive cells on the brain were identified by dark-brown staining under light microscopy.

Assessment of BBB permeability by Evans blue dye staining

BBB integrity damage in mice was checked by Evans blue dye staining as previously described with minor modification [17]. In brief, mice in different groups received a tail vein injection of Evans blue dye (2% in PBS, 4 ml/kg body weight) for 30 min. After being euthanized by i.p. injection of pentobarbital sodium, the left ventricle was perfused with 20 mL of heparin saline to remove intravascular-localized Evans blue dye. The brain tissue was excised, photographed, weighed, and placed in 20 ml of formamide at 60°C for 24 h to extract the Evans blue dye. Formamide supernatant was harvested by centrifugation at 1,000 rpm for 5 min and read at 620 nm using a Model Microplate Reader (iMark, Bio-Rad). The amount of extracted Evans Blue dye was determined in comparison to standard curves and expressed as ng/mg of tissue weight.

Western blotting for ZO-1 and Claudin-5 protein in brain tissue

The protein levels of ZO-1 and Claudin-5 in brain tissues were analyzed in different groups using western blotting assay. In brief, proteins in brain tissue were extracted in RIPA lysis buffer (Beyotime, China) and quantitated using BCA kit assay (Beyotime, China). The protein supernatants from each sample were separated using a 10% SDS-PAGE gels and subsequently electroblotted onto a polyvinylidene difluoride (PVDF) membrane. The membranes were blocked with 5% non-fat milk at 37°C for 2 h and then subsequently exposed to the specific primary antibodies (anti-ZO-1 or anti-Claudin-5; BD Biosciences, USA) overnight at 4°C, followed by incubation with horseradish peroxide enzyme-conjugated goat anti-rabbit immunoglobulin G (1/2000; ab6721) at 37 °C for 1 h. The target bands were visualized and analyzed using an ECL chemiluminescent detection system (Amersham, USA). β-actin protein was used as the internal control.

bEnd.3 cell viability assay

The effect of MCs-Exo on bEnd.3 cells viability were performed using CCK-8 assay. The bEnd.3 cells were purchased from the Cell Bank of Chinese Academy of Sciences (Shanghai, China), and cultured in DMEM medium (GIBCO, No.12800017) containing $NaHCO_3$ (1.5g/L), FBS (10%), penicillin (100 U/mL), and streptomycin (100 μg/mL) in 75-cm^2 tissue culture flasks at 37 °C in 5% CO_2 and 95% air atmosphere. When the cells attained a density of 10^6 cells/mL, the bEnd.3 cells were plated in 96-well plates (10^4 cells/well). The cells were immediately incubated with *Pb*Ag (20 μg/mL), MCs-Exo (50 μg/mL), and *Pb*Ag (20 μg/mL) plus MCs-Exo (50 μg/mL), respectively. As the MCs-Exo and/or *Pb*Ag were suspended in complete medium, and alternatively flasks were added into only complete medium as blank control. At 24 h, 48 h, and 72 h after incubation, the bEnd.3 cells from different groups were then incubated with 10 μL CCK-8 (Beyotime Biotechnology, China) for 1 h at 37 °C, and the absorbance of each well was measured at 450 nm using a Model Microplate Reader (iMark, Bio-Rad).

Quantitative qPCR assay

To assess the effect of MCs-Exo on the expression of ZO-1, Claudin-5, Ang-1, and Ang-2, as well as the release of chemokines (CCL2, CXCL1, and CXCL9) from bEnd.3 cells stimulated with *Pb*Ag, qPCR assay was performed. When the cells attained a density of 10^6 cells/mL in 75-m^2 plate, the bEnd.3 cells were plated in 6-well plates (10^4 cells/well). *Pb*Ag (20 μg/mL), MCs-Exo (50 μg/mL), and *Pb*Ag (20 μg/mL) plus MCs-Exo (50 μg/mL) were immediately put into bEnd.3 cells, respectively. After 48 h, total RNA of bEnd.3 cells in different groups were harvested using with Trizol reagent (TaKaRa, Japan), quantitated by using a 1.0% agarose gel, and subsequently quantified by determining the ration of absorbance at 260 nm to 280 nm with a NanoDrop 2000 spectrophotometer (NanoDrop Technologies, USA). cDNA was synthesized from 1.0 μg of total RNA by using PrimeScript 1 st Strand cDNA Synthesis Kit (TaKaRa, Japan), and stored at −80 °C until use. To measure the mRNA expression of CCL2, CXCL1, CXCL9, Ang-1, Ang-2, ZO-1 and Claudin-5 in bEnd.3 cells, the SYBR Green qPCR Master Mix (TaKaRa, Japan) was used to perform qPCR reaction with a Lightcycler®480 instrument (Roche Diagnostics, Switzerland). The qPCR reactions were constructed in a total volume of 10 μL mixture comprising 5.0 μL of SYBR® Premix Ex Taq TM (2×), 0.5 μL of forward- or reverse-primer (10 pM), 1.0 μL of cDNA template (100 ng/μL), and 3.0 μL of ddH_2O according to the manufacturer's instructions. The qPCR reaction contained 95°C for 30 s, 43 cycles of 95°C for 5 s and 60°C for 20 s. The Primer sequences used in this study were listed as follows: ZO-1, 5'-GAACGCTCTCATAAGCTTCGTAA-3' (forward) and 5'- ACCGTACCAACCATCATTCATTG-3' (reverse); Claudin-5, 5'-TCTGCTGGTTCGCCAACAT-3' (forward), and 5'-CGGCACCGTCGGATCA-3'

(reverse); Ang-1, 5'-TGCAGCAACCAGCGCCGAAA-3' (forward) and 5'-CAG GGCAGTTCCCGTCGTGT-3' (reverse); Ang-2, 5'-GCTTCGGGAGCCCTCTGGGA-3' (forward) and 5'-CAGCGAATGCGCCTCGTTGC3' (reverse); CCL2, 5'-GCAGCAGGTG

TCCCAAAGAA-3' (forward) and 5'-GGTCAGCACAGACCTCTCTCTTG-3' (reverse);

CXCL1, 5'-CCACACTCAAGAATGGTCGC-3' (forward) and 5'-TCTCCGTTACTTGG

GGACAC-3' (reverse); CXCL9, 5'-GAACTCAGCTCTGCCATGAA-3'(forward) and 5'-GCATCGTGCATTCCTTATCA-3' (reverse);β-actin, 5'-GTGCTATGTTGCTCTAGAC

TTCG-3 (forward) and 5'-ATGCCACAGGATTCCATACC-3' (reverse). The mRNA levels of target genes were normalized to those of β-actin gene, and the results were indicated as the fold amplification in comparison to those of naive controls by using $2^{-\Delta\Delta CT}$ method.

Statistical analysis

All data are reported as the mean ± SEM. Statistical analysis of data was carried out using GraphPad Prism 5 software. Statistical significance between two experimental groups was assessed using the Independent Sample t-test. Log-Rank test, a time-series analysis test, or one-way ANOVA was used to

evaluate the significance difference among multiple groups. $P<0.05$ was considered statistically significant.

Results

Identification and distribution of MCs-Exo

MCs-Exo were extracted from the culture supernatants of *Pb*Ag stimulated P815 cells using commercial kit, and characterized quality, morphology, and size by using negative-staining TEM, western blotting, and NanoSight assays, respectively. Negative-staining TEM analysis showed that MCs-Exo displayed closed round like vesicles with a typical diameter of 30–150 nm (Fig. 1A). Western blotting analysis revealed that the exosomal markers including CD9, CD81, and CD63 were positively expressed in MCs-Exo (Fig. 1B). Furthermore, NanoSight analysis indicated that the size of diameter in MCs-Exo ranged from 30 to 150 nm, with a peak of 86 nm (Fig. 1C). To track the *in vivo* distribution of MCs-Exo in mice, DiR-labeled MCs-Exo were i.v. injected into the uninfected C57BL/6 mice. As expected, *in vivo* fluorescence imaging showed that the DiR-labeled MCs-Exo were mainly detected in liver, spleen, and brain tissues (Fig. 2A), while rarely localized in the heart, kidney, or lung tissues after 6 h of i.v. injection. Similarly, *ex vivo* images of dissected organs at 6 h post-injection showed that DiR-labeled MCs-Exo was predominantly taken up by the liver, spleen, and brain tissues (Fig. 2B), but not other tissues (Data without show). These findings confirmed that MCs-Exo were successfully extracted from the culture supernatant of *Pb*Ag-treated P815 cells and mainly transmitted into liver, spleen, and brain tissues of mice *via* i.v. injection.

MCs-Exo shorten host survival time and elevated incidence of ECM

To determine the effect of MCs-Exo on *Pb*ANKA-mediated pathogenesis, *Pb*ANKA-infected mice were received daily i.v. injection of MCs-Exo (50 μg/mouse, *Pb*+MCs-Exo group) or saline (*Pb* group). The *Pb*ANKA-infected control mice died between 6 to 16 days p.i., while the infected mice with MCs-Exo treatment had shorter host survival time and 100% of mortality by day 6 to 9 p.i. (Fig. 3A). Mice showing neurological impairments manifestations (ECM mice) were found in both *Pb* and *Pb*+MCs-Exo groups, and were usually moribund within 6-9 days p.i.. Importantly, the incidence of ECM in *Pb*+MCs-Exo group was much higher than those in *Pb* group (100% *vs* 70%, $P<0.01$). However, no significance of peripheral parasitemia in *Pb*ANKA-infected mice was observed in *Pb* group and *Pb*+MCs-Exo group on days 3–9 p.i. ($P > 0.05$ in all the time points; Fig. 3B). These findings indicated that MCs-Exo treatment could boost *Pb*ANKA-infected mice from ECM.

ECM mice have more MCs and remain higher level of MCs degranulation

In uninfected mice with saline (Naïve group) or MCs-Exo (MCs-Exo group) treatment, only a few or rare number of positively stained-MCs (including intact and degranulated MCs) were found to locate in major tissues (e.g., skin, cervical lymph node, and brain). While MCs were obviously detected in tissues

mentioned above from ECM mice selected in both *Pb* and *Pb*+MCs-Exo group (Fig. 4A). Compared with uninfected control mice (Naïve group), MCs number was elevated in skin (~4 cells/mm^2 *vs* ~12 cells/mm^2, $P < 0.01$), cervical lymph node (~2 cells/mm^2 *vs* ~15 cells/mm^2, $P < 0.01$), and brain (~0.5 cells/mm^2 *vs* ~6 cells/mm^2, $P < 0.01$) tissues of ECM mice selected in *Pb* group (Fig. 4B). Similarly, the higher levels of degranulated MCs in skin (~10% *vs* ~75%, $P < 0.01$), cervical lymph node (~8% *vs* ~68%, $P < 0.01$), and brain (~4% *vs* ~50%, $P < 0.01$) tissues were observed from ECM mice selected in *Pb* group in comparison to those from Naïve mice (Fig. 4C). However, there was no significant difference in MCs number ($P > 0.05$) or levels of degranulated MCs ($P > 0.05$) in skin, cervical lymph node, or brain tissues of ECM mice selected in *Pb* and *Pb*+MCs-Exo groups.

MCs-Exo exacerbated liver and brain damage in ECM mice

Given that MCs-Exo were successfully transmitted into liver and brain tissues of mice after 6 h of i.v. injection, we evaluated whether MCs-Exo alter histopathological change of liver and brain from ECM mice. As shown in Fig. 5A, H&E staining showed that no obvious inflammatory foci were detected in liver tissue from uninfected mice treated with saline (Naïve group) or MCs-Exo (MCs-Exo group). However, severe damage with obvious inflammatory foci were observed in liver tissue of ECM mice selected in *Pb* group (Fig. 5A-b, 5C). Remarkably, the administration of MCs-Exo led to more severe damage and higher number of inflammatory foci in liver tissue from ECM mice ($P < 0.01$, Fig. 5A-d, 5C). Similarly, serum concentrations of AST and ALT in mice were also determined by ELISA assay (Fig. 5D and 5E), and the data showed that a significant increase in sera AST ($P = 0.0041$) and ALT ($P = 0.0252$) from ECM mice selected in *Pb*+MCs-Exo group related to those in *Pb* group.

H&E staining also showed no obvious signals of inflammation or iRBCs sequestration were observed in brain tissues in Naïve or MCs-Exo group (Fig. 5B). As expected, ECM mice selected in *Pb* group obviously exhibited moderate iRBCs sequestration, leukocyte infiltration in the parenchymal and pia vessels, and multifocal hemorrhages (Fig. 5B-b). The administration of MCs-Exo accumulated more mononuclear cells, higher iRBCs sequestration in cerebral blood vessels, and even resulted in more obvious hemorrhage in the brain tissues from ECM mice (Fig. 5B-d). To further investigate vascular integrity, the numbers of hemorrhage sites per file were quantified in brain tissues from different groups. Compared with ECM mice selected in *Pb* group, ECM mice selected in *Pb*+MCs-Exo group remain much more hemorrhage sites (Fig. 5F). These findings further confirmed that MCs-Exo aggravated liver and brain damage in ECM mice.

MCs-Exo promoted Th1 cytokine responses in ECM mice

To determine whether MCs-Exo alter Th1 cytokine response in ECM mice, ELIAS assay was performed to analyze the protein levels of Th1 cytokines in sera among different groups. As shown in Fig. 6, there was no significant change in protein levels of IFN-γ ($P > 0.05$), TNF-α ($P > 0.05$), IL-1α ($P > 0.05$), or IL-6 ($P > 0.05$) among uninfected mice treated with saline (Naïve group) and MCs-Exo (MCs-Exo group). However, compared with uninfected control mice (Naïve group), protein levels of IFN-γ ($P = 0.0004$), TNF-α ($P <$

0.0001), IL-1α ($P < 0.0001$), and IL-6 ($P = 0.0011$) increased in sera from ECM mice selected in *Pb* group. Notably, there was increase of IFN-γ ($P = 0.0116$), TNF-α ($P = 0.0241$), IL-1α ($P = 0.0012$), and IL-1β ($P = 0.0250$) of ECM mice selected in *Pb*+MCs-Exo group in comparison to those in *Pb* group.

MCs-Exo promoted BBB leakage in ECM mice

Considering that BBB disruption is the most important feature of ECM mice [10], Evans blue permeability assay was used to evaluate whether MCs-Exo alter BBB integrity in ECM mice. As shown in Fig. 7A, Evans blue dye cannot leave into the brain parenchyma in mice from Naïve (Fig. 7A-a) or MCs-Exo group (Fig. 7A-c), whereas the breakdown of BBB was obviously observed in ECM mice selected in *Pb* (Fig. 7A-b) and *Pb*+MCs-Exo (Fig. 7A-d) groups, as demonstrated by Evans blue dye cross into the brain parenchyma. ECM mice selected in *Pb*+MCs-Exo group showed raised levels of Evans blue dye penetration by ~1.2 fold related to those in *Pb* group (~73.7 ng/mg *vs* ~85.5 ng/mg, $P = 0.0074$; Fig. 7B). Similarly, the levels of BBB permeability markers (ZO-1 and Claudin-5) were detected from different groups by western blotting assay (Fig. 7C, 7D, and 7E). Our data showed that lower expression of ZO-1 ($P = 0.0132$) and Claudin-5 ($P = 0.0131$) in brain tissue of ECM mice selected in *Pb*+MCs-Exo group than those in *Pb* group. Together, these results suggested that MCs-Exo could play an aggravating role in BBB damage during ECM development.

MCs-Exo triggered brain vascular endothelial activation in ECM mice

Given that vascular endothelial activation impairs endothelial function and BBB integrity, and thus is used as a hallmark feature of ECM pathology [10], immunohistochemistry for ICAM-1 and VCAM-1 were performed to assess whether MCs-Exo can trigger vascular endothelial activation in brain tissues of ECM mice. As shown in Fig. 8, no or only a few ICAM-1- and VCAM-1- positively stained cells were observed in the brain tissue of uninfected mice treated with saline (Naïve group) or MCs-Exo (MCs-Exo group), while there were obvious positive cells with ICAM-1 and VCAM-1 expression in brain tissues from ECM mice selected in both *Pb* and *Pb*+MCs-Exo groups. Further analysis showed that higher integrated optical density (IOD) of ICAM-1 ($P = 0.0014$) and VCAM-1 ($P = 0.0415$) protein expression were detected in ECM mice selected in *Pb*+MCs-Exo group in comparison to those in *Pb* group. These results demonstrated that the MCs-Exo play a role in triggering brain vascular endothelial activation in ECM mice.

MCs-Exo exacerbated the decline of bEnd.3 cells viability upon *Pb*Ag, and promoted endothelial activation *in vitro*

We next investigated the effect of MCs-Exo on bEnd.3 cells viability upon *Pb*Ag stimulation *in vitro* using CCK8 assay. As shown in Fig. 9, under complete medium condition, MCs-Exo had no obvious effect on bEnd.3 cells viability and did not cause any cytotoxicity in bEnd.3 cells *in vitro*. After *Pb*Ag stimulation, the OD value was reduced by ~25% ($P < 0.0001$) or ~21% ($P < 0.0001$) at 48 h or 72 h *in vitro*, respectively. *Pb*Ag co-cultured with MCs-Exo led to decrease of OD value by ~22% ($P = 0.0027$) or ~15% ($P = 0.0113$) at 48 h or 72 h in related to those with only *Pb*Ag stimulation, respectively. Compared with Naive group, qPCR assay showed that *Pb*Ag treatment upregulated the mRNA levels of Ang-2 ($P <$

0.0001), CCL2 ($P < 0.0001$), CXCL1 ($P < 0.0001$), and CXCL9 ($P < 0.0001$), whereas downregulated level of Ang-1 ($P = 0.0001$), ZO-1 ($P = 0.0001$) and Claudin-5 ($P < 0.0001$) in bEnd.3 cells (Fig. 10). Moreover, the treatment of MCs-Exo resulted in increase of the mRNA levels of Ang-2 ($P = 0.0008$), CCL2 ($P = 0.0066$), CXCL1 ($P < 0.0001$), and CXCL9 ($P = 0.0014$), whereas led to the decline of the Ang-1 ($P = 0.0012$), ZO-1 ($P = 0.0156$), and Claudin-5 ($P = 0.0008$) mRNA levels in bEnd.3 cells of *Pb*Ag+MCs-Exo group. Collectively, these results indicated that MCs-Exo could exacerbate the decline of bEnd.3 cells viability with *Pb*Ag treatment, and promote endothelial activation *in vitro*.

Discussions

In the present study, we assess whether MCs-Exo trigger pathogenesis of ECM by i.v. injecting MCs-Exo into *Pb*ANKA-infected C57BL/6 mice (a widely-used and exclusive model of ECM) and surveilling the bEnd.3 cells upon the MCs-Exo treatment after *Pb*Ag stimulation. Our finding demonstrated that the MCs-Exo treatment dramatically elevated the ECM incident in *Pb*ANKA-infected mice, which could be partly mediated by aggravating brain pathology damage, brain vascular endothelial activation and BBB disruption. Therefore, our data suggested that MCs-Exo promote pathogenesis of ECM.

The present study showed that exosomes were found to secrete from P815 cells after *Pb*Ag stimulation, as demonstrated by rounded structures with a size of 30-150 nm by TEM and NanoSight assays, and a positive expression of traditional exosome markers (CD9, CD81, and CD63) by western blotting assay. Our data is consistent with the description of exosomes based on size and morphology, as previous reports showing that several kinds of MCs can constitutively release exosomes [30]. Although Intra-cerebroventricular (ICV) injection is widely used in the field of brain function research, this injection could unavoidably harm structure and function of brain to a certain extent. To determine whether MCs-exosomes transmit into major tissues, we adopted i.v injection rather than ICV injection of MCs-Exo into mice in this study. Our data demonstrated that after 6 h of i.v. injection, DiR-labeled MCs-Exo were successfully transmitted into liver and brain tissues through *in vivo* and *ex vivo* tracking.

Our previous report demonstrated that i.p. injection of MCs-degranulating agent (C48/80) did not alter ECM incidence or BBB disruption in *Pb*ANKA-infected Kunming mice [17]. One possibility could be that Kunming mice with *Pb*ANKA infection may not be an ideal ECM model, although only one study reported that 100% of *Pb*ANKA-infected Kunming mice develop into ECM [36]. In the present study, ECM mice exhibited higher MCs density and higher percentage of MCs degranulation in various tissues (skin, cervical lymph node, and brain) in comparison to naive mice, which is similar to those in previous reports [16,17]. Since several kinds of MCs can constitutively release exosomes [30], it is reasonably supposed that MCs-Exo could be mediate the ECM severity. To investigate the functional effect of MCs-Exo on ECM pathogenies, we used an exclusive ECM murine model (C57BL/6 mice infected with *Pb*ANKA) instead of Kunming mice infected with *Pb*ANKA. Our finding showed only ~80% but not 100% of *Pb*ANKA-infected C57BL/6 mice developed into ECM, maybe due to different cloned lines of *Pb*ANKA that was found to relate with the extent of ECM induction [37]. Further study demonstrated that i.v. injection of MCs-Exo

dramatically increased the incident of ECM changed from ~80% to 100% in the present study, suggesting that MCs-Exo treatment could boost *Pb*ANKA-infected mice from ECM.

The outcome of malaria severity was found to relate with a delicate balance between pro- and anti-inflammatory immune responses. Although pro-inflammatory immune responses can control the early phase of malaria infection, but they play an immunopathology role in CM severity [38]. Recent studies have revealed that pro-inflammatory cytokines (e.g., IFN-γ, TNF-α, IL-6, and IL-1α) play a critical role in driving the immunopathological process leading to ECM by using *Pb*ANKA-infected gene knockout C57BL/6 mice [38]. To investigate the effect of MCs-Exo on Th1 cytokine responses in ECM mice, the protein levels of TNF-α, IFN-γ, IL-6, and IL-1α in sera were measured from different groups. Our data showed that MCs-Exo notably elevated the levels of TNF-α, IFN-γ, IL-6, and IL-1α in ECM mice. Our data is contrast to previous report where bone marrow-derived mast cells (BMMCs)-derived exosomes dramatically promoted the differentiation of naïve CD4+ T cells to Th2 cells *via* OX40L-OX40 ligation [39]. Thus, our data suggested that the MCs-Exo may aggravate the development of ECM through production and secretion of pro-inflammatory cytokines. However, the present study did not accurately elucidate what kind of cells triggered by MCs-Exo was responsible for the elevated levels of cytokines (e.g., TNF-α, IFN-γ, IL-6, and IL-1α).

The BBB integrity acts as an important elements of central nervous system homeostasis, that is critical to minimize local inflammation and neuronal damage [9]. Several previous studies indicated MCs were found to mainly locate close to blood vessels on the brain side of the BBB, and implicated in the pathogenesis of neurodegenerative diseases via mediating BBB changes integrity [40-42]. In course of *Plasmodium* infection, the disruption of BBB integrity was obviously detected in CM patients and ECM mice, as indicated by hemorrhages in brains of CM patients and extravasation of Evan blue dye, cytokines or antibodies into the brain parenchyma in ECM mice [43]. Further analysis demonstrated BBB disruption was recognized as a central hallmark of ECM, and contributed to the appearance of long-term neurological signs in the survivors from CM [10]. In this study, we found that i.v injection of MCs-Exo dramatically promoted the disruption of BBB integrity in ECM mice, as provided that more Evan blue dye leakage into brain parenchyma, and lower protein levels of tight junction proteins (ZO-1 and Claudin-5). Our data is similarly to other report that plasma exosomes in children with obstructive sleep apnea led to the disruption of BBB integrity [44]. Meanwhile, brain metastatic breast cancer cells-derived exosomes breach integrity of BBB by transferring lncRNA GS1-600G8.5 [45]. Contrarily, pericyte-derived exosomes improved microcirculation and the endothelial ability to regulate blood flow, and protected blood-spinal cord barrier after spinal cord injury in mice [46]. It was known that endothelial activation and dysfunction may progress to loss of BBB integrity in ECM mice [43]. In the present study, our data furtherly demonstrated that MCs-Exo can elevate the protein expression biomarkers of endothelial activation and dysfunction (such as VCAM-1 and VCAM-1) in brain tissue of ECM mice by immunohistochemistry. Similarly, activated monocyte-derived exosome activated brain endothelial activation *via* altering TLR4/MyD88 pathway [47]. In the present study, an *in vitro* study also demonstrated MCs-Exo notably exacerbate the decline of bEnd.3 cells viability upon *Pb*Ag and elevated the ration of Ang-2, whereas decreased the mRNA levels of Ang-1, ZO-1, and Claudin-5 in bEnd.3 cells upon *Pb*Ag. Our data is similarly

to other report that co-culture with *P. falciparum*-infected erythrocytes, human endothelial cell lines were reported to upregulate ICAM-1 expression [48,49]. Thus, our data suggesting that i.v injection of MCs-Exo could promote development of ECM in *Pb*ANKA-infected mice, maybe due to trigger BBB disruption and endothelial activation.

Apart from iRBC sequestration, leukocytes accumulations are also found in the cerebral microvasculature in ECM mice or CM patients [50]. Further analysis indicated that chemokines secreted from several types of cells could initiate and amplify a local inflammatory response, which in turn enhances further leukocyte recruitment, thereby was associated with CM severity [51]. A serial study was demonstrated that CCL2 acted as a powerful attractant of monocytes trafficking, CXCL1 served as a factor in neutrophil trafficking, while CXCL9 trafficked T cell and NK cell to inflammatory sites [51]. In this study, our data showed that the treatment of MCs-Exo led to a significant elevate in the mRNA levels of CCL2, CXCL1, and CXCL9 in bEnd.3 cells upon *Pb*Ag *in vitro*. Our data is similar to the previous reports that upon co-culture with *Pb*Ag, bEnd.3 cells were reported to increase transcription of CXCL1 and to secrete MCP-1/CCL2 [48,52,53]. Thus, our data suggest that elevated mRNA levels of CCL2, CXCL1, and CXCL9 in bEnd.3 cells after MCs-Exo stimulation may be contribute to the recruitment of leukocyte in microvasculature during ECM development.

Conclusion

In summary, the data presented here demonstrated that i.v. injection of MCs-Exo shortened host survival time, while exacerbated brain histopathological damage, and elevated incidence of ECM in *Pb*ANKA-infected C57BL/6 mice. Our data provided evidences that MCs-Exo may contribute to pathogenesis of ECM, maybe due to enhancing pro-inflammatory response in host, promoting brain microvascular endothelial cells activation and BBB breakdown. Our finding will provide new insights into the roles of MCs-Exo in ECM pathogenesis in mice. However, it remains to be proven the exclusive mechanism how MCs-Exo trigger endothelial cells activation or BBB breakdown during ECM development.

Declarations

Acknowledgements

Not applicable

Funding

This work was financially supported by the National Natural Science Foundation of China (No. 81702020), National Students' Platform for Innovation and Entrepreneurship Training Program (No. 201910573003), and Innovation and University Promotion Project of Guangdong Pharmaceutical University (No. 2017KCXTD020). The funds had no role in study design, data collection and analysis, decision to publish, or preparation of the manuscript.

Author Contributions

BH and ZL designed the experiments. KH, XZ, LH, HL, ZY, XL, XBL, QW, YW, JW, and XJ performed experiments. BH and ZL analyzed data, wrote and revised the manuscript. XH, HG, RL, and SC revised the manuscript. All authors read and approved the final manuscript.

Ethics declarations

Ethics approval and consent to participate

The experimental protocols were performed with the approval of the Animal Ethics Committee of Guangdong Pharmaceutical University (No. gdpulac2020023), and confirmed to the National Guidelines for the Care and Use of Laboratory Animals.

Consent for publication

Not applicable.

Competing interests

The authors declare that they have no competing interests.

Availability of data and materials

The data supporting the conclusions of this article are available within the article.

References

1. WHO. World Malaria Report 2018. 2019, Geneva: World Health Organization.
2. Ghazanfari N, Mueller S, Heath W. Cerebral malaria in mouse and man. Front Immunol. 2018; 9:2016.
3. Datta D, Conroy A, Castelluccio P, Ssenkusu J, Park G, Opoka R, et al. Elevated cerebrospinal fluid tau protein concentrations on admission are associated with long-term neurologic and cognitive impairment in Ugandan children with cerebral malaria. Clin Infect Dis. 2020; 70:1161–1168.
4. Amimo F, Lambert B, Magit A. What does the COVID-19 pandemic mean for HIV, tuberculosis, and malaria control? Trop Med Health. 2020; 48:32.
5. Chiodini J. COVID-19 and the impact on malaria. Travel Med Infect Dis. 2020; 35: 101758.
6. Menard D, Dondorp A. Antimalarial drug resistance: a threat to malaria elimination. Cold Spring Harb Perspect Med. 2017; 7:a025619.
7. Su X, Lane K, Xia L, Sá J, Wellems T. Plasmodium genomics and genetics: new insights into malaria pathogenesis, drug resistance, epidemiology, and evolution. Clin Microbiol Rev. 2019; 32: e00019.
8. Matuschewski K. Vaccines against malaria-still a long way to go. FEBS J. 2017; 284:2560–2568.

9. Chow B, Gu C. The molecular constituents of the blood-brain barrier. Trends Neurosci. 2015; 38:598–608.
10. Nishanth G, Schlüter D. Blood-brain barrier in cerebral malaria: pathogenesis and therapeutic intervention. Trends Parasitol. 2019; 35:516–528.
11. González-de-Olano D, Álvarez-Twose I. Mast cells as key players in allergy and inflammation. J Investig Allergol Clin Immunol. 2018; 28:365–378.
12. Mukai K, Tsai M, Starkl P, Marichal T, Galli S. IgE and mast cells in host defense against parasites and venoms. Semin Immunopathol. 2016; 38:581–603.
13. Marshall J, Portales-Cervantes L, Leong E. Mast cell responses to viruses and pathogen products. Int J Mol Sci. 2019; 20: 4241.
14. Lu F, Huang S. The Roles of Mast Cells in Parasitic Protozoan Infections. Front Immunol. 2017; 8:363.
15. Porcherie A, Mathieu C, Peronet R, Schneider E, Claver J, Commere P, et al. Critical role of the neutrophil-associated high-affinity receptor for IgE in the pathogenesis of experimental cerebral malaria. J Exp Med. 2011; 208:2225–2236.
16. Wilainam P, Nintasen R, Viriyavejakul P. Mast cell activation in the skin of Plasmodium falciparum malaria patients. Malar J. 2015; 14, 67.
17. Huang B, Huang S, Chen X, Liu X, Wu, Q, Wang Y, et al. Activation of mast cells promote *Plasmodium berghei* ANKA infection in murine model. Front Cell Infect Microbiol. 2019; 9:322.
18. Furuta T, Kikuchi T, Iwakura Y, Watanabe N. Protective roles of mast cells and mast cell-derived TNF in murine malaria. J Immunol. 2006; 177, 3294–3302.
19. Chau J, Tiffany C, Nimishakavi S, Lawrence J, Pakpour N, Mooney J, et al. Malaria-associated L-arginine deficiency induces mast cell-associated disruption to intestinal barrier defenses against nontyphoidal Salmonella bacteremia. Infect Immun. 2013; 81:3515–3526.
20. Guermonprez P, Helft J, Claser C, Deroubaix S, Karanje H, Gazumyan A, et al. Inflammatory Flt3l is essential to mobilize dendritic cells and for T cell responses during Plasmodium infection. Nat Med.2013; 19:730–738.
21. Potts R, Tiffany C, Pakpour N, Lokken K, Tiffany C, Cheung K, et al. Mast cells and histamine alter intestinal permeability during malaria parasite infection. Immunobiology. 2016; 221:468–474.
22. Theoharides T, Kempuraj D, Tagen M, Conti P, Kalogeromitros D. Different release of mast cell mediators and the pathogenesis of inflammation. Immunol. 2007; 217:65–78.
23. Samanta S, Rajasingh S, Drosos N, Zhou Z, Dawn B, Rajasingh J. Exosomes: new molecular targets of diseases. Acta Pharmacol Sin. 2018; 39:501–513.
24. Sampaio N, Cheng L, Eriksson E. The role of extracellular vesicles in malaria biology and pathogenesis. Malar J. 2017; 16:245.
25. Debs S, Cohen A, Hosseini-Beheshti E, Chimini G, Hunt N, Grau G. Interplay of extracellular vesicles and other players in cerebral malaria pathogenesis. Biochim Biophys Acta Gen Subj. 2019;

1863:325–331.

26. de Souza W, Barrias E. Membrane-bound extracellular vesicles secreted by parasitic protozoa: cellular structures involved in the communication between cells. Parasitol Res. 2020; 119: 2005–2023.
27. Mantel P, Hoang A, Goldowitz I, Potashnikova D, Hamza B, Vorobjev I, et al. Malaria infected erythrocyte-derived microvesicles mediate cellular communication within the parasite population and with the host immune system. Cell Host Microbe. 2013; 13: 521–534.
28. Mantel P, Hjelmqvist D, Walch M, Kharoubi-Hess S, Nilsson S, Ravel D, et al. Infected erythrocyte-derived extracellular vesicles alter vascular function via regulatory Ago2-miRNA complexes in malaria. Nat Commun. 2016; 7:12727.
29. Martin-Jaular L, Nakayasu E, Ferrer M, Almeida I, A Del Portillo H. Exosomes from Plasmodium yoelii-infected reticulocytes protect mice from lethal infections. PLoS One. 2011; 6:e26588.
30. D'Incà F, Pucillo C. Exosomes: tiny clues for mast cell communication. Front Immunol. 2015; 6:73.
31. Huo C, Wu H, Xiao J, Meng D, Zou S, Wang M, et al. Genomic and bioinformatic characterization of mouse mast cells (P815) upon different influenza a virus (H1N1, H5N1, and H7N2) infections. Front Genet. 2019; 10:595.
32. Skokos D, Le Panse S, Villa I, Rousselle J, Peronet R, David B, et al. Mast cell-dependent B and T lymphocyte activation is mediated by the secretion of immunologically active exosomes. J Immunol. 2001; 166:868–876.
33. Chen B, Li Y, Guo Y, Zhao X, Lim H. Mast cell-derived exosomes at the stimulated acupoints activating the neuro-immune regulation. Chin J Integr Med. 2017; 23: 878–880.
34. Xie G, Yang H, Peng X, Lin L, Wang J, Lin K, et al. Mast cell exosomes can suppress allergic reactions by binding to IgE. J Allergy Clin Immunol. 2018; 141:788–791.
35. Xiao H, He M, Xie G, Liu Y, Zhao Y, Ye X, et al. The release of tryptase from mast cells promote tumor cell metastasis via exosomes. BMC Cancer. 2019; 19:1015.
36. Ding Y, Xu W, Zhou T, Liu T, Zheng H, Fu Y. Establishment of a murine model of cerebral malaria in KunMing mice infected with *Plasmodium berghei* ANKA. Parasitology. 2016; 143:1672–1680.
37. Amani V, Boubou M, Pied S, Marussig M, Walliker D, Mazier D, et al. Cloned lines of *Plasmodium berghei* ANKA differ in their abilities to induce experimental cerebral malaria. Infect Immun. 1998; 66:4093–4099.
38. Engwerda C, Good M. Interactions between malaria parasites and the host immune system. Curr Opin Immunol. 2005; 17:381–387.
39. Li F, Wang Y, Lin L, Wang J, Xiao H, Li J, et al. Mast cell-derived exosomes promote Th2 cell differentiation via OX40L-OX40 ligation. J Immunol Res. 2016; 2016: 3623898.
40. Skaper S, Facci L, Giusti P. Mast cells, glia and neuroinflammation: partners in crime? Immunology. 2014; 141:314–327.

41. Jones M, Nair A, Gupta M. Mast Cells in Neurodegenerative Disease. Front Cell Neurosci. 2019; 13:171.
42. Kempuraj D, Mentor S, Thangavel R, Ahmed M, Selvakumar G, Raikwar S, et al. Mast cells in stress, pain, blood-brain barrier, neuroinflammation and alzheimer's Disease. Front Cell Neurosci. 2019; 13:54.
43. Rénia L, Howland S, Claser C, Charlotte Gruner A, Suwanarusk R, Hui T, et al. Cerebral malaria: mysteries at the blood-brain barrier. Virulence. 2012; 3:193–201.
44. Khalyfa A, Gozal D, Kheirandish-Gozal L. Plasma exosomes disrupt the blood-brain barrier in children with obstructive sleep apnea and neurocognitive deficits. Am J Respir Crit Care Med. 2018; 197:1073–1076.
45. Lu Y, Chen L, Li L, Cao Y. Exosomes derived from brain metastatic breast cancer cells destroy the blood-brain barrier by carrying lncRNA GS1-600G8.5. Biomed Res Int. 2020; 2020:7461727.
46. Yuan X, Wu Q, Wang P, Jing Y, Yao H, Tang Y, et al. Exosomes derived from pericytes improve microcirculation and protect blood-spinal cord barrier after spinal cord injury in Mice. Front Neurosci. 2019; 13:319.
47. Dalvi P, Sun B, Tang N, Pulliam L. Immune activated monocyte exosomes alter microRNAs in brain endothelial cells and initiate an inflammatory response through the TLR4/MyD88 pathway. Sci Rep. 2017; 7:9954.
48. Viebig N, Wulbrand U, Forster R, Andrews K, Lanzer M, Knolle P. Direct activation of human endothelial cells by *Plasmodium falciparum*-infected erythrocytes. Infect Immun. 2005; 73:3271–3277.
49. Tripathi A, Sullivan D, Stins M. *Plasmodium falciparum* infected erythrocytes increase intercellular adhesion molecule 1 expression on brain endothelium through NF-kappaB. Infect Immun. 2006; 74:3262–3270.
50. Pai S, Qin J, Cavanagh L, Mitchell A, El-Assaad F, Jain R, et al. Real-time imaging reveals the dynamics of leukocyte behaviour during experimental cerebral malaria pathogenesis. PLoS Pathog. 2014; 10:e1004236.
51. Dunst J, Kamena F, Matuschewski K. Cytokines and chemokines in cerebral malaria pathogenesis. Front Cell Infect Microbiol. 2017; 7:324.
52. Tripathi A, Sha W, Shulaev V, Stins M, Sullivan D. *Plasmodium falciparum*-infected erythrocytes induce NF-kappaB regulated inflammatory pathways in human cerebral endothelium. Blood. 2009; 114:4243–4252.
53. Chakravorty S, Carret C, Nash G, Ivens A, Szestak T, Craig A. Altered phenotype and gene transcription in endothelial cells, induced by Plasmodium falciparum-infected red blood cells: pathogenic or protective? Int J Parasitol. 2007; 37:975–987.

Figures

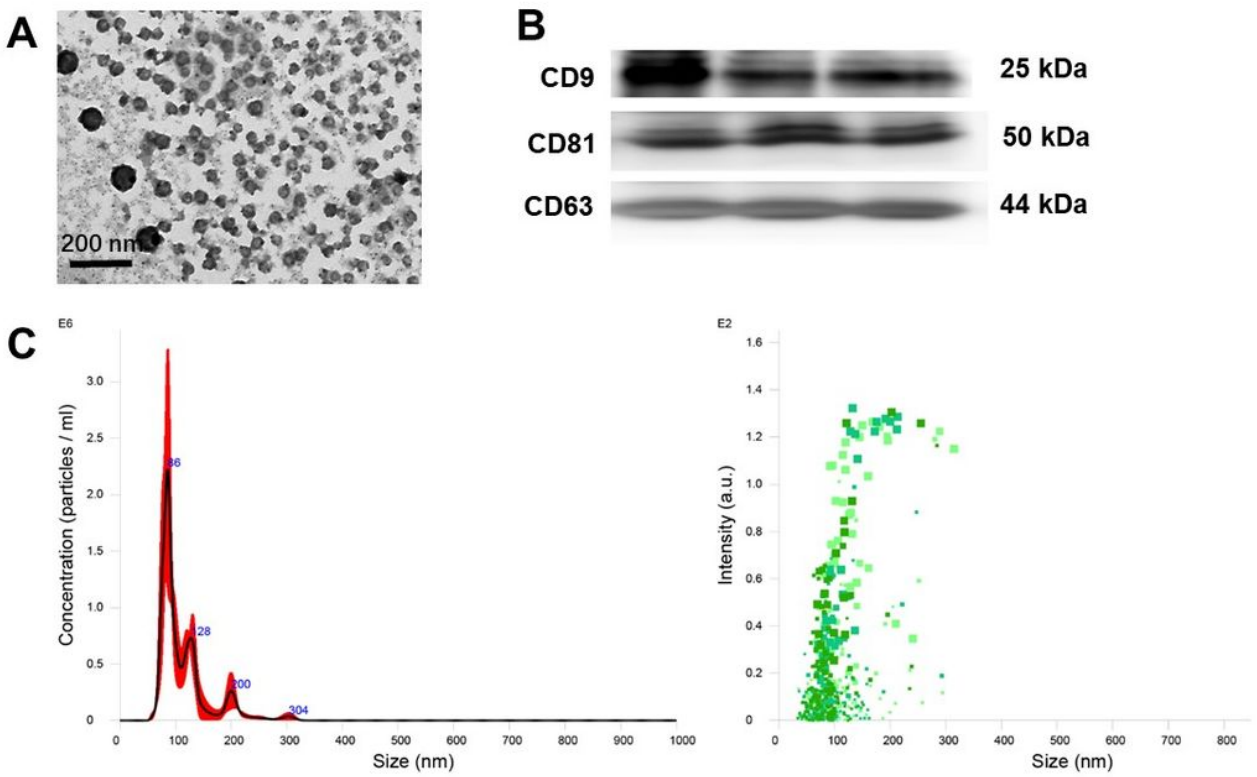

Figure 1

Characterization of MCs-Exo. (A) MCs-Exo displayed closed round like vesicles with a typical diameter of 30–150 nm by TEM; (B) MCs-Exo had a positive expression of exosomal markers, including CD9, CD81, and CD63 by Western blot analysis; (C) The size and the concentration of MCs-Exo was analyzed using NanoSight NS300.

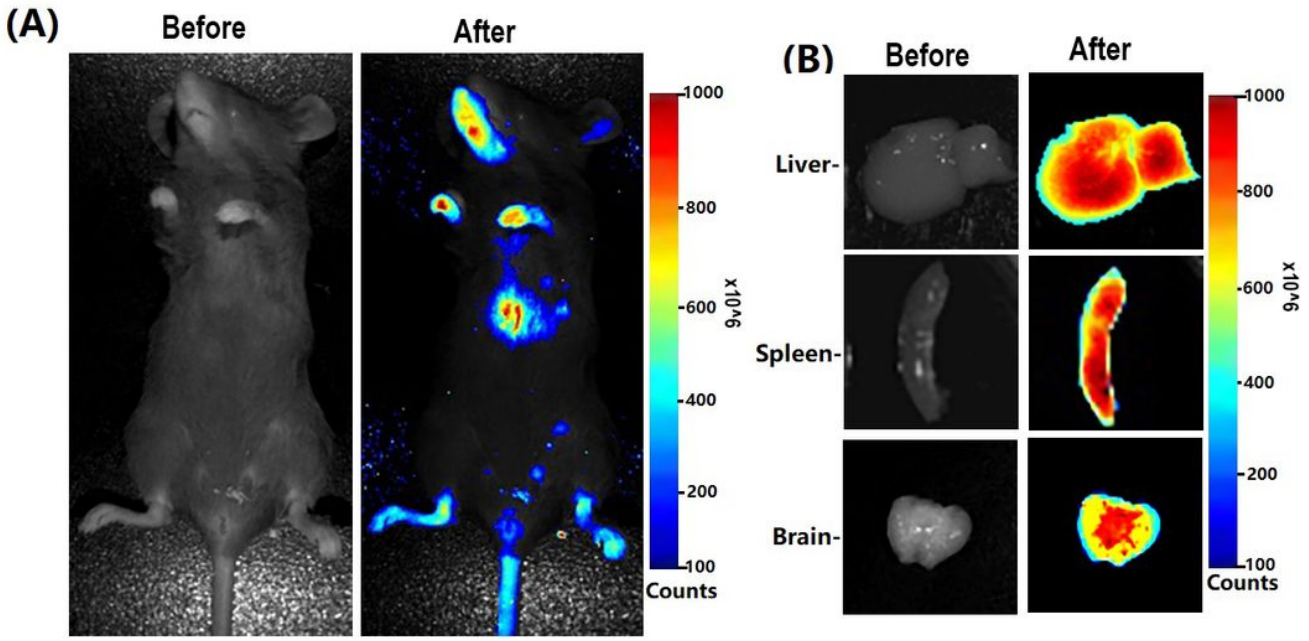

Figure 2

In vivo and ex vivo fluorescence imaging of DiR-labeled MCs-Exo in mice after 6 h of i.v. injection. The naïve C58BL/6 mice received i.v. injection of DiR-labeled MCs-Exo to verify the distribution of MCs-Exo in mice and dissected organs. (A) Living animals were imaged by using the Maestro2 In-Vivo Imaging System at 0 h and 6 h of i.v. injection; (B) Representative fluorescence images of dissected organs (liver, spleen, and brain) of mice sacrificed at 0 h and 6 h after i.v. injection of DiR-labeled MCs-Exo.

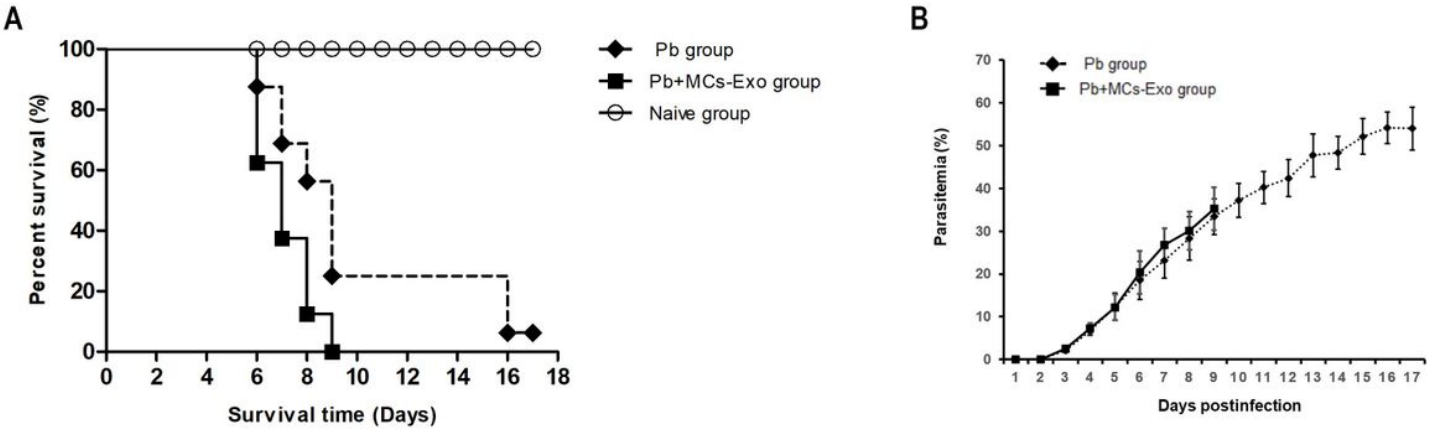

Figure 3

The survival time and parasitemia detected in PbANKA-infected mice with or without MCs-Exo treatment. The C57BL/6 mice were i.p. infected with 106 PbANKA-iRBCs, and then received daily i.v. injection of MCs-Exo (50 μg/mouse) or equal volume of saline. (A) These mice were evaluated daily regarding survival time; (B) Parasitemia in different groups was monitored daily by Giemsa-stained thin blood smears of tail blood. This experiment was repeated three times, and the data were represented as mean ± SEM. Log-Rank test or a time-series analysis test was used to evaluate the significance difference in survival time or parasitemia, respectively. Statistical significance of ECM incidence in PbANKA-infected mice was assessed between Pb group and Pb+MCs-Exo group using Independent Student's t-test.

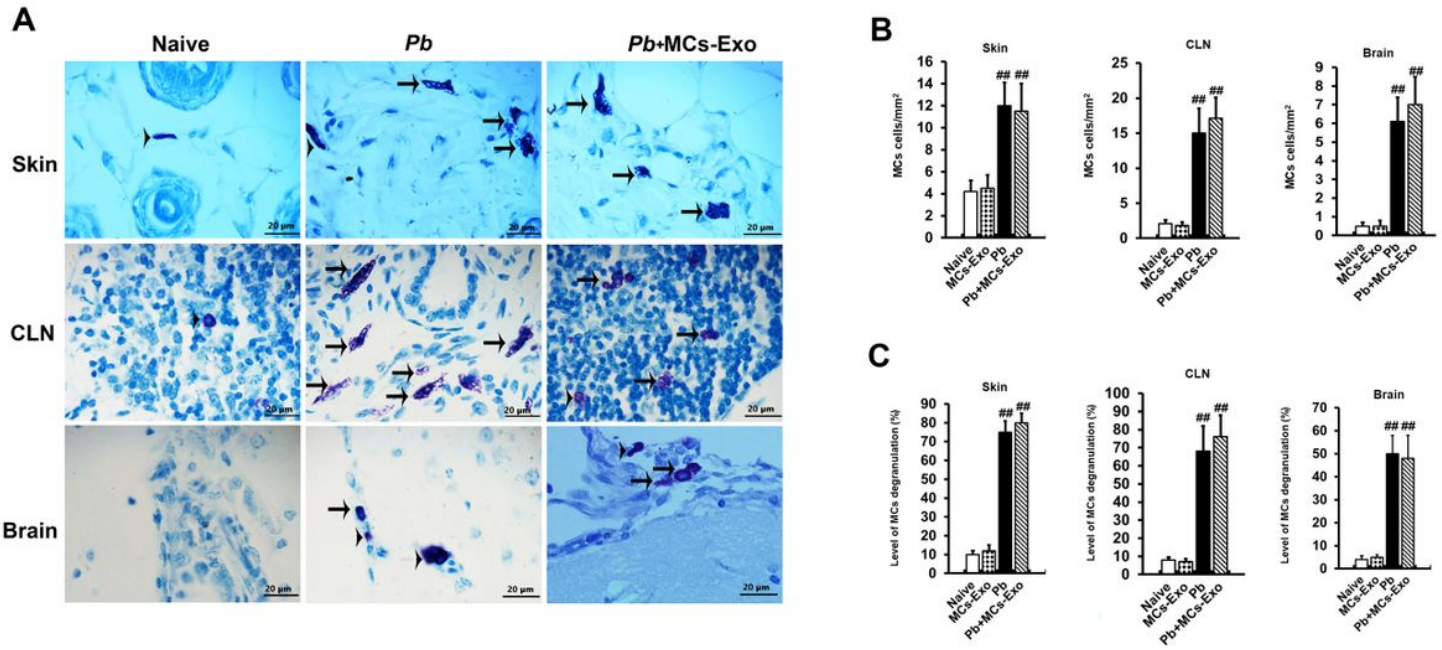

Figure 4

Elevated MCs number and level of MCs degranulation in major tissues from ECM mice. (A) Toluidine blue staining was used to evaluate MCs in skin, cervical lymph node (CLN), or brain tissues from naïve mice or ECM mice randomly selected from Pb and Pb+MCs-Exo groups. Degranulated MCs (arrows). Intact MCs (arrowheads); (B) and (C) Statistical significance of MCs number/mm2 and the level of MCs degranulation in section of skin, CLN, or brain tissue were determined among multiple groups using a one-way ANOVA followed by Dunnett's multiple comparison test versus Naïve group (#P < 0.05 and ##P < 0.01). Statistical significance between two experimental groups was determined using the Independent Student's t-test analysis (*P < 0.05 and **P < 0.01 vs. Pb group).

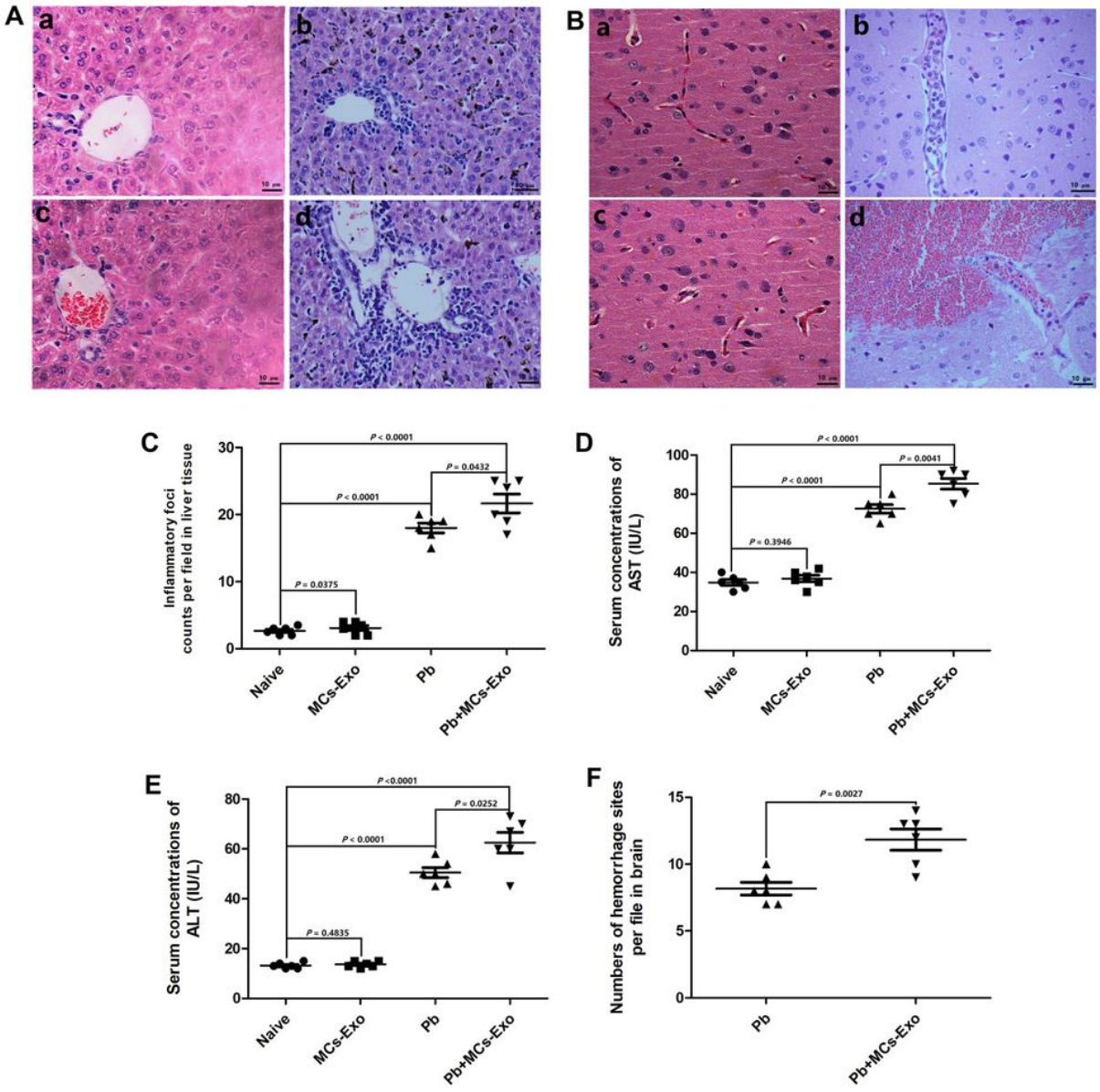

Figure 5

MCs-Exo exacerbated liver and brain damage in ECM mice. (A,B) The C57BL/6 mice were i.p. infected with 106 PbANKA-iRBCs, and then received daily i.v. injection of MCs-Exo (50 μg/mouse) or equal volume of saline. ECM mice was randomly selected in Pb and Pb+MCs-Exo groups, and histopathology in liver or brain was evaluated by H&E staining (magnification, x400). Naive mice (a); ECM mice selected in Pb group (b); uninfected mice treated with MCs-Exo (c); ECM mice selected in Pb+MCs-Exo group (d). (C,D,E) Histopathological scores in liver tissues (or inflammatory foci per field), and serum concentrations of AST

and ALT were determined in mice. Statistical significance between two experimental groups was determined using the Independent Student's t-test analysis.

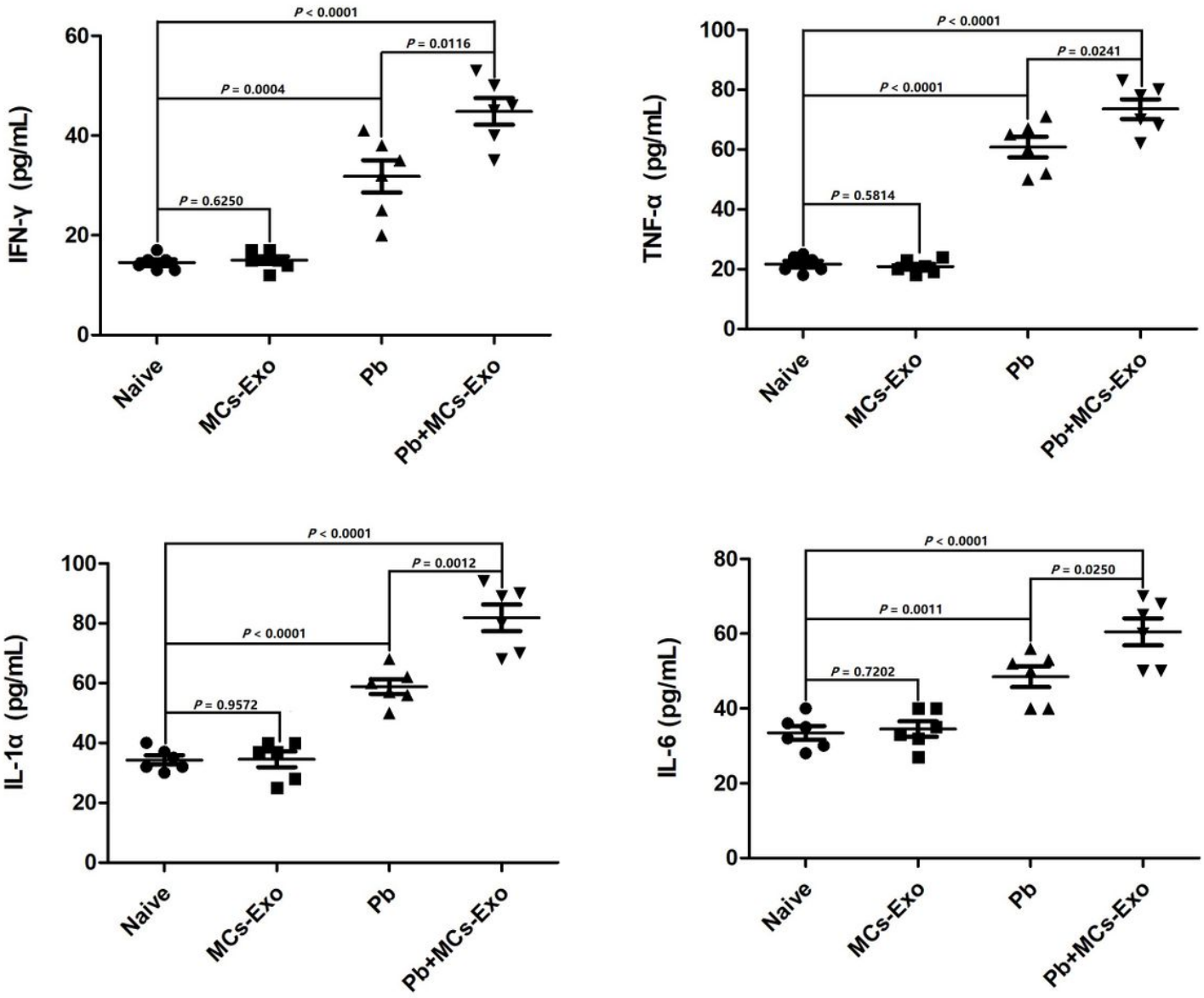

Figure 6

MCs-Exo promoted Th1 cytokine responses in sera of ECM mice. The C57BL/6 mice were i.p. infected with 106 PbANKA-iRBCs, and then received daily i.v. injection of MCs-Exo (50 μg/mouse) or equal volume of saline. Sera were collected from ECM mice from Pb and Pb+MCs-Exo groups, and determined for TNF-α, IFN-γ, IL-1α, and IL-6 by ELISA assay. Statistical significance between two experimental groups was determined using the Independent Student's t-test analysis.

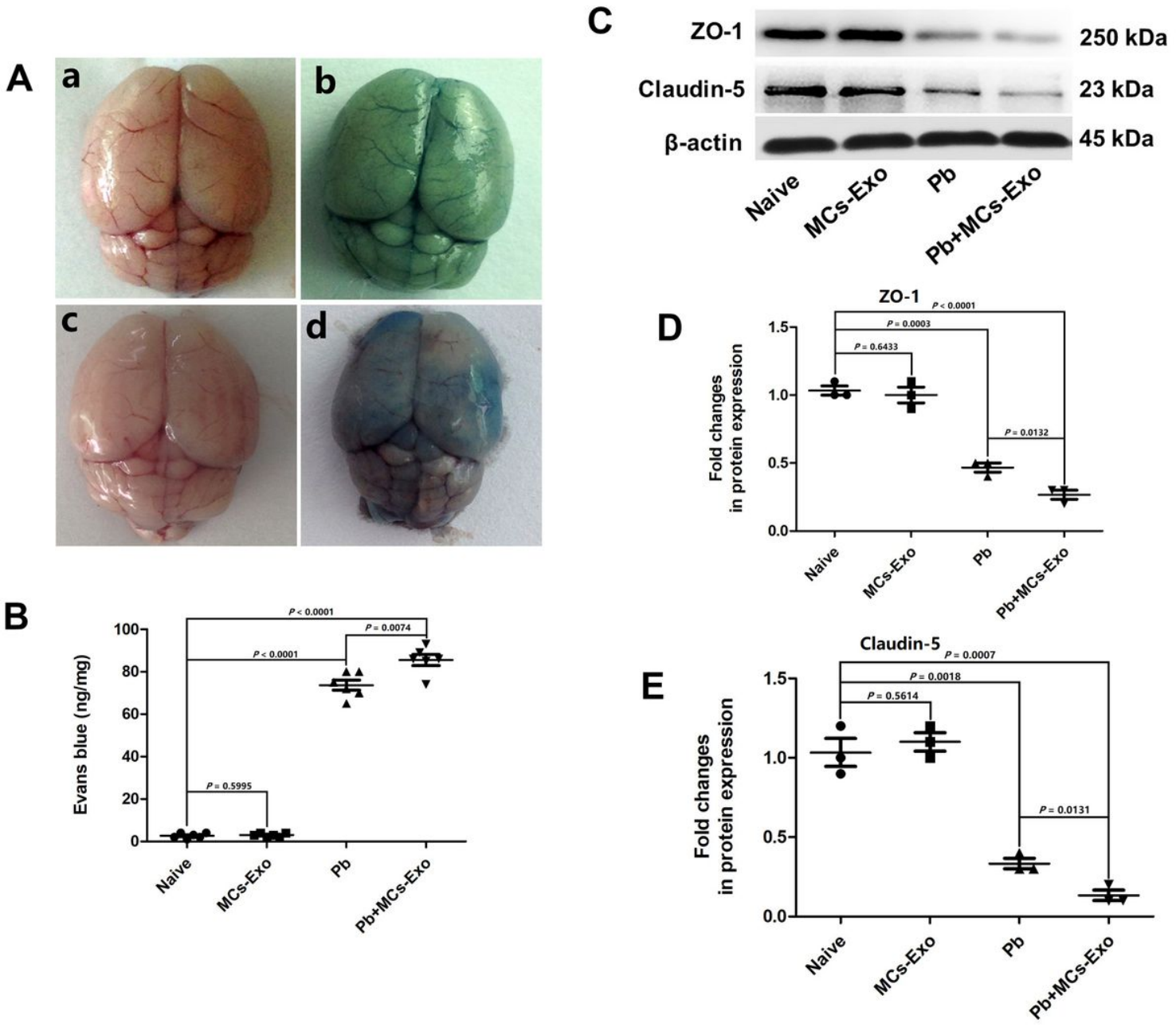

Figure 7

MCs-Exo exacerbated BBB leakage in ECM mice. To assess vascular damage in brain tissue by MCs-Exo, Evans blue dye was i.v. injected into Naïve mice, uninfected mice with MCs-Exo treatment (MCs-Exo group), ECM mice randomly selected from Pb and Pb+MCs-Exo groups (n = 6/group). (A) Photographs of representative image of brain from different group. (B) Quantitation of Evans blue dye extravasation in brains and the amount of extracted Evans Blue dye was determined in comparison to standard curves and expressed as ng/mg of brain tissue weight. (C) Western blotting assay was performed to assess ZO-1 and Claudin-5 protein expression in the brain tissue of mice. Statistical significance between two experimental groups was analyzed using the Independent Student's t-test analysis.

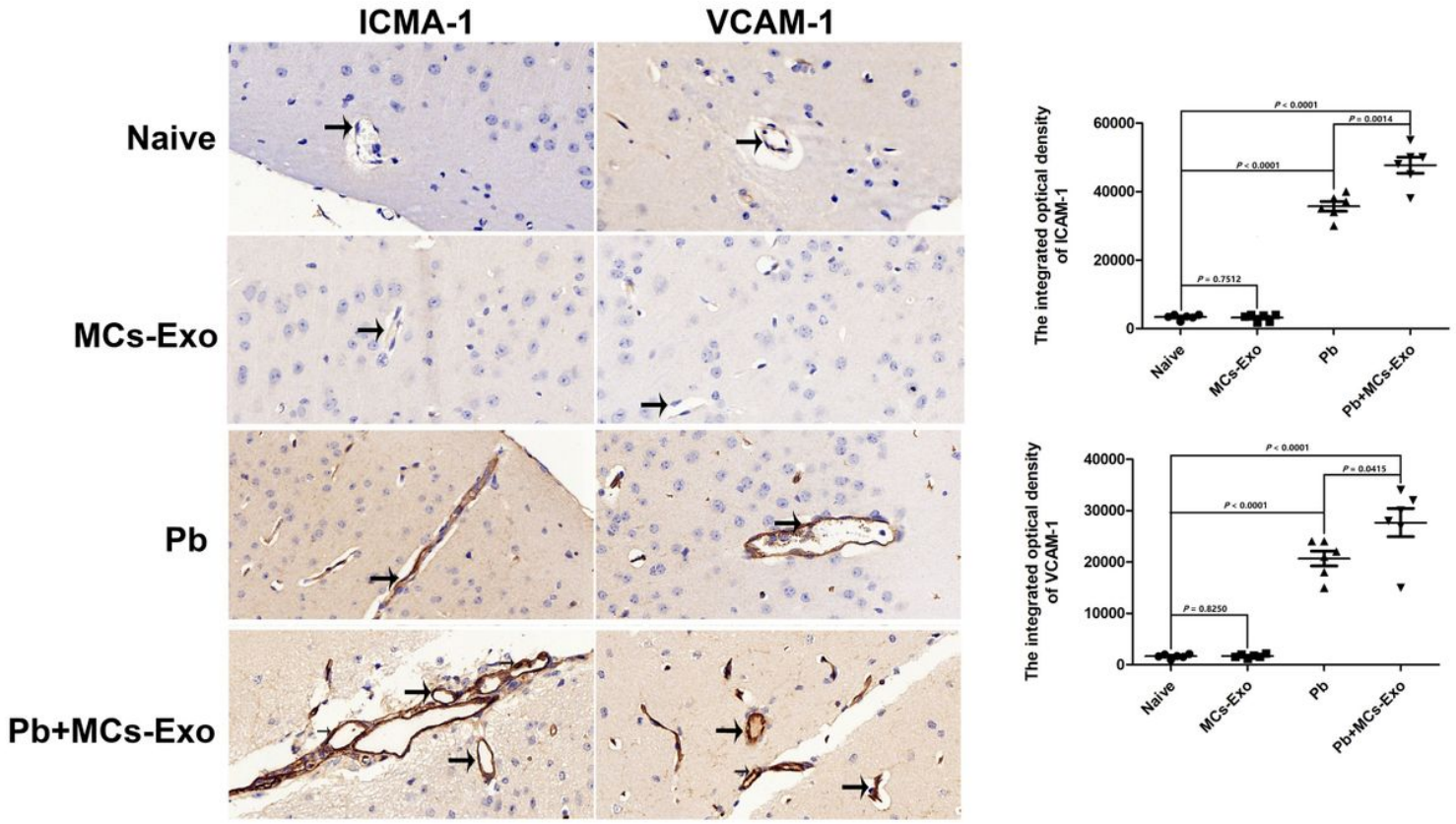

Figure 8

MCs-Exo promoted brain vascular endothelial activation in ECM mice. (A) Immunohistochemistry analysis of ICAM-1 and VCAM-1 protein expression in the brain tissue from Naïve mice, uninfected mice with MCs-Exo treatment (MCs-Exo group), ECM mice randomly selected from Pb and Pb+MCs-Exo groups (n = 6/group). (B) The integrated optical density (IOD) of ICAM-1 and VCAM-1 protein expression in brain tissue was analyzed among different groups. Statistical significance between two experimental groups was analyzed using the Independent Student's t-test analysis.

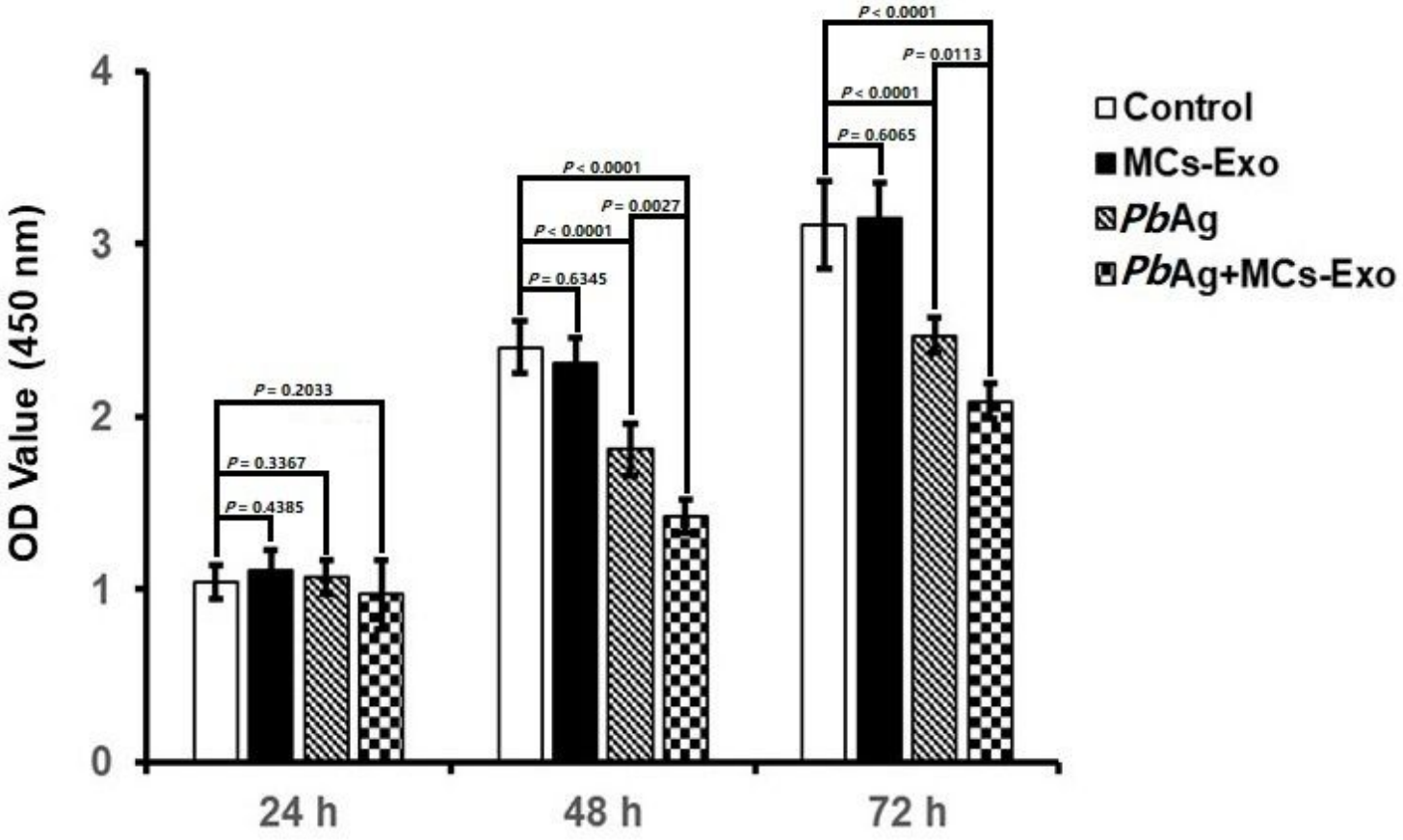

Figure 9

The effect of MCs-Exo on the viability of bEnd.3 cells upon PbAg with or with MCs-Exo at 24 h, 48 h, and 72 h in vitro. Data are reported as the mean ± SEM. Statistical significance between two experimental groups was analyzed using the Independent Student's t-test analysis.

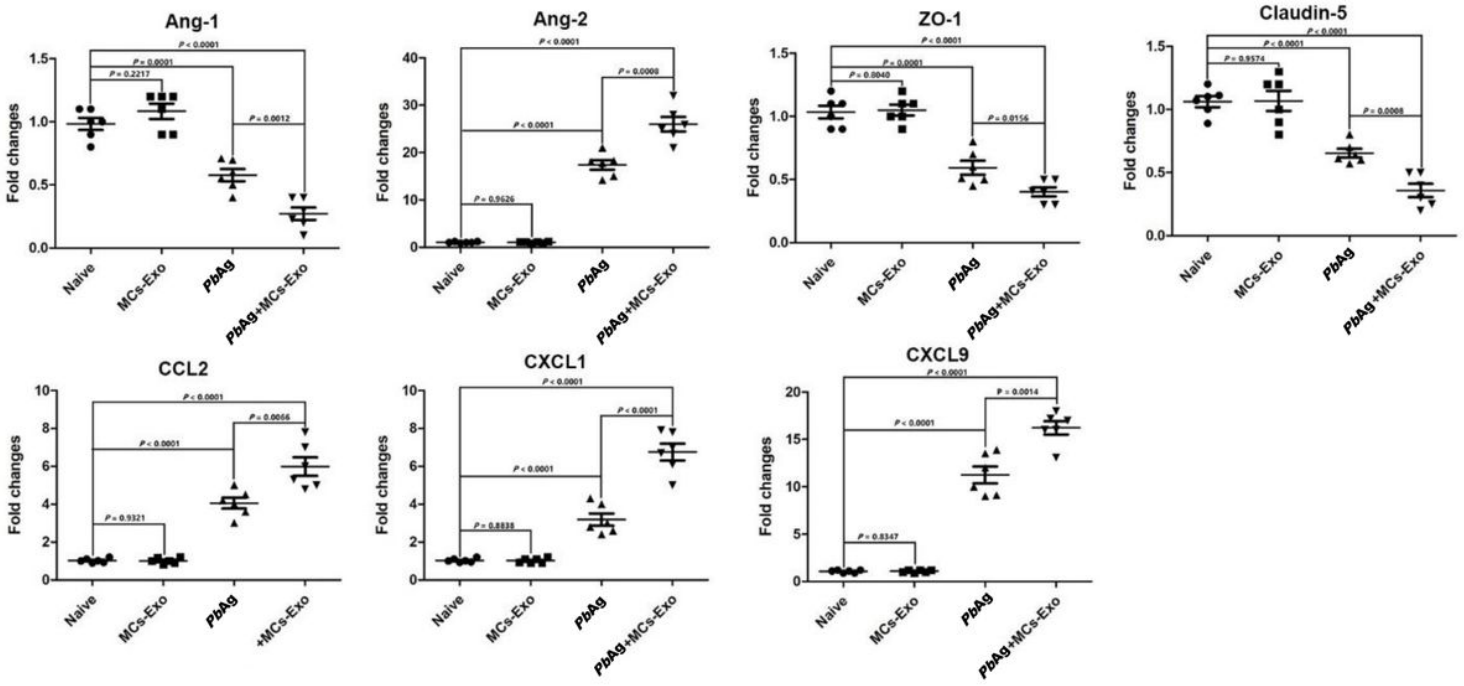

Figure 10

The relative mRNA expressions of Ang-1, Ang-2, ZO-1, Claudin-5, CCL2, CXCL1, and CXCL9 in bEnd.3 cells upon PbAg with or with MCs-Exo in vitro using qPCR assay. The bEnd.3 cells plated in 6-well plates were cultured PbAg, MCs-Exo, PbAg plus MCs-Exo for 48h, respectively. The mRNA levels of target genes were normalized to β-actin gene, and the results were indicated as the fold amplification in comparison to those of naive controls by using 2-ΔΔCT method. Statistical significance between two experimental groups was analyzed using the Independent Student's t-test analysis.

Supplementary Files

This is a list of supplementary files associated with this preprint. Click to download.

- GraphicalAbstract.pdf